Journal of Robotics and Control (JRC)
Volume 5, Issue 3, 2024
ISSN: 2715-5072, DOI: 10.18196/jrc.v5i3.21366

Model Predictive Control Design under Stochastic Parametric Uncertainties Based on Polynomial Chaos Expansions for F-16 Aircraft

Heri Purnawan [1], Tahiyatul Asfihani [2*], Seungkeun Kim [3], Subchan Subchan [4]
[1, 2, 4] Department of Mathematics, Institut Teknologi Sepuluh Nopember, Surabaya, Indonesia
[1] Department of Electrical Engineering, Universitas Islam Lamongan, Lamongan, Indonesia
[3] Department of Aerospace Engineering, Chungnam National University, Daejeon, Republic of Korea
Email: [1] heripurnawan@unisla.ac.id, [2] t_asfihani@matematika.its.ac.id, [3] skim78@cnu.ac.kr, [4] subchan@matematika.its.ac.id
*Corresponding Author

***Abstract*—Parametric uncertainty in a dynamical system has the potential to undermine the performance of a closed-loop controller designed through classical techniques. This paper presents a novel approach to stochastic model predictive control (SMPC) by employing the polynomial chaos expansion (PCE) method called PCE-based model predictive control (PCE-MPC). This method offers a more robust and efficient solution to tackle parameter uncertainties in dynamic systems. The PCE method is utilized to propagate uncertainties through orthogonal polynomials, and the Galerkin projection approach is employed to compute PCE coefficients via intrusive spectral projection (ISP). In Galerkin projection, the inner product involves an integration term, and the integration values are approximated using the Gauss-Legendre quadrature. This quadrature method precisely integrates the p-th order polynomial using $2p-1$ points. The numerical case study focuses on the short-period mode of the F-16 aircraft model. Simulation results demonstrate the robust performance of the proposed method in the presence of parameter uncertainties, with system states converging to the original points for each parameter realization under various initial conditions. Comparison results indicate negligible differences between MPC and PCE-MPC, showcasing nearly identical performance. However, further investigation is warranted in other cases and more complex systems involving parameter uncertainties.**

***Keywords*—Galerkin Projection; Intrusive Spectral Projection; Parameter Uncertainty; Polynomial Chaos; SMPC.**

I. INTRODUCTION

The exploration of control system design, taking into account parameter uncertainties in dynamical systems, has emerged as an exciting research area [1]–[5]. The impact of parametric uncertainty becomes apparent when a controller is designed using classical techniques such as Proportional, Integral, Derivative (PID), and Linear Quadratic Regulator (LQR) [6]–[8], potentially leading to the deterioration of closed-loop performance. In the aerospace field, parameter uncertainties can arise from inaccuracies in aerodynamic coefficient modeling [9]. The need to address uncertainties in designing control algorithms arises particularly when dealing with known physical systems.

According to [10], parametric uncertainty emerges in systems where the underlying physics is known, but the system parameters are either imprecisely known or anticipated to fluctuate over the operational lifetime. This uncertainty is also present when constructing system models from experimental data through system identification techniques, representing a system plant with an unknown parameter transfer function. Experimental measurements result in parameter values within a range of uncertainty. In both scenarios, the assumed knowledge is the variation range of these parameters, and the objective is to design controllers that ensure specified performance across these variations.

Addressing parameter uncertainties effectively involves the use of robust control strategies [11]–[16]. In these control strategies, a worst-case analysis is performed to assess how variations in parameters impact the robustness of the control system. As a result, these strategies may be excessively cautious, especially when parameters rarely reach extreme values [17]. To mitigate this, adopting a control design approach that takes into account the distribution of parameters is expected to be less conservative. A novel way to implement the robust control concept is through stochastic control, where the uncertainty related to system parameters is acknowledged to follow a probability distribution [18]–[20]. By leveraging the understanding of the uncertainty distribution in system parameters, a control system designer may be willing to accept a modest yet clearly defined level of risk to achieve more substantial robustness margins.

A crucial aspect in stochastic control involves handling the time evolution of uncertainty within model equations, essentially simulating stochastic systems. The widely used Monte Carlo is a common method for simulating general stochastic systems. However, its utility in control design may be constrained by the significant computational complexity involved. An efficient tool to significantly reduce the computational workload needed for simulating a stochastic system is Polynomial Chaos Expansion (PCE). This method utilizes the orthogonal polynomials, which are functions of random variables to approximate the uncertain parameters and the system states [21], [22]. In addition, the PCE framework was applied to solve some problems in engineering, such as fluid dynamics [23]–[25], finite elements [26]–[28], and solid mechanics [29]–[32]. The primary challenge in PCE is how to determine the coefficients of polynomial expansion. Typically, two methods, Galerkin projection and collocation [33], [34], can be employed to determine the coefficients of expansion. The

collocation method matches a PCE to the model output using uncertainty samples basically utilizing interpolation and regression [35], while the Galerkin projection method obtains a PCE by projecting the model output onto the space spanned by basis functions. Collocation has drawbacks, such as the lack of a well-established best way to select samples and the fact that the approximation error controlled by collocation does not necessarily decrease with the addition of more samples. The Galerkin method has two versions: intrusive and non-intrusive spectral projections [36]–[38]. The Intrusive Spectral Projection (ISP) approach has the advantage of being a more rigorous way for calculating PCE coefficients compared to the Non-Intrusive Spectral Projection (NISP) [39]. However, the limitations of this method are when the model is changed the whole code must be rewritten and tailored for every case and to solve the inner product is not straightforward for nonlinear systems. Another issue is the dimension system will be larger than the original system [40]. Despite its drawbacks, this approach is a straightforward method for designing control systems using models formulated in a state space equation.

The application of PCE has been integrated with several control system methods, as demonstrated in references [3], [10], [17]–[20], [41]–[43] and therein. In [17], Linear Quadratic (LQ) control is designed by considering an expanded state space due to parameter variations using PCE. The expansion of the state space is achieved by transforming the probabilistic system into a deterministic one using the Galerkin method through the ISP approach. To efficiently handle high-order stochastic approximations, a modified LQ control is introduced for gain selection and performance evaluation [44]. This adaptation of LQ control exhibits improved performance for systems characterized by probabilistic uncertainty. However, it is important to note that the LQ control lacks the inclusion of input and state constraints in the design process, which may lead to potential constraint violations.

To overcome the limitations associated with handling applications where there is a cost advantage in either violating constraints or closely approaching operational limits, a burgeoning area of research focuses on the development of an advanced control system known as Stochastic Model Predictive Control (SMPC) [45]–[47]. SMPC commonly employs random sampling techniques like Monte Carlo [48], [49], where the system model is simulated multiple times based on samples to predict the time evolution of uncertainties. Despite its applicability to a range of problems, sampling-based approaches can become prohibitively expensive due to the substantial number of samples needed for accurate uncertainty propagation.

In response to the limitations of Monte Carlo-based SMPC, an effective alternative is to use Polynomial Chaos Expansion-based Model Predictive Control (PCE-MPC). Numerous studies on PCE-MPC for systems with parameter uncertainties are documented in various literatures, as seen in references [50]–[53]. It is worth noting that the referenced papers assume the independence of randomness in parameter uncertainties. Building on insights from those works, our paper contributes as follows.

1) Design PCE-MPC by assuming the parameter uncertainties are not independent but are instead regulated by a single random variable.
2) Develop a generalized mapping from a stochastic to a deterministic linear system using an efficient approach to handle parameter uncertainties in dynamical systems. In contrast the approach presented in [10], we consider the system input to be deterministic.
3) Present an optimization for SMPC reformulated as a deterministic MPC problem through the utilization of the PCE method.

The proposed method is applied to the F-16 aircraft using a linear state space equation. To solve the PCE-MPC optimization problem, we utilize the quadratic programming (QP) method [54]–[56]. This method is widely used for addressing quadratic cost functions while accommodating linear equality and inequality constraints.

The structure of this work is presented as follows. Firstly, Section 2 explores the theoretical underpinnings of PCE, setting the stage for our novel approach. Then, the PCE-MPC optimization problem constructed from the SMPC using the PCE method is expressed in Section 3. Additionally, Section 3 presents the formula of the PCE-MPC problem in the QP framework. Next, the numerical example to implement the proposed method and discussion results is given in Section 4. Lastly, the end section of this paper draws the conclusion and suggestions that can be implemented in the future.

II. UNCERTAINTY QUANTIFICATION

This section explains PCE theory and its application to derive linear systems with time-invariant probabilistic uncertainties to be deterministic linear systems.

A. Polynomial Chaos Expansion for One-dimensional Space

Firstly, Wiener proposed the PCE to approximate the Gaussian random variables using polynomial expansions [57]. The polynomial chaos utilizes an orthogonal basis of $\mathcal{L}_2(\Omega, \mathcal{F}, \rho)$, where $\mathcal{L}_2(\Omega, \mathcal{F}, \rho)$ is the probability space of all random events ξ with finite variance. The probability space $(\Omega, \mathcal{F}, \rho)$ is defined on the basis of the Ω sample space, σ-algebra $\mathcal{F}$, and the probability size ρ on $(\Omega, \mathcal{F})$. A random variable, $v(\xi) \in \mathcal{L}_2(\Omega, \mathcal{F}, \rho)$, has the expansion [58]:

$$v(\xi) = \sum_{m=0}^{\infty} c_m \, \phi_m(\xi), \tag{1}$$

where c_m indicates the deterministic expansion coefficient and $\phi_m(\xi)$ represents the PCEs basis which depends on the random variable vector ξ. The selection of the basis for the polynomial is adjusted to the random variable distribution. In fact, the convergence rate strongly depends on the basis selection [59], [60].

The expansion in Eq. (1) should be truncated for implementation. Thus, the expansion after truncation can be written as (2) [61].

$$v(\xi) \approx \tilde{v}(\xi) = \sum_{m=0}^{p} c_m \, \phi_m(\xi) = \boldsymbol{c}^T \, \bar{\boldsymbol{\phi}}(\xi), \tag{2}$$

where $\boldsymbol{c} = [c_0, c_1, \cdots, c_p]^T$, $\bar{\boldsymbol{\phi}}(\xi) = [\phi_0, \phi_1, \cdots, \phi_p]^T$ with p is the order of polynomial basis function. For a one-dimensional PCE, the number of terms is $p+1$. After the coefficient $\boldsymbol{c}$ in (2) is calculated, the property of the orthogonal polynomial can be utilized to calculate the statistical measures of the random variable $\tilde{v}(\xi)$ especially to know the accuracy of PCE in predicting mean and variance.

To determine the polynomial basis in PCEs, Table I gives a piece of information on how to select the polynomial ϕ_m corresponding to the probability density function (pdf) of random variable ξ [40].

TABLE I. THE ORTHOGONAL POLYNOMIAL OF DIFFERENT PROBABILITY DENSITY FUNCTION FOR CONTINUOUS RANDOM VARIABLES

Polynomial $\phi_m(\xi)$	Random Variable ξ	Domain
Hermite	Gaussian	$(-\infty, \infty)$
Legendre	Uniform	$[-1, 1]$
Jacobi	Beta	$(-1, 1)$
Laguerre	Gamma	$(0, \infty)$

B. Intrusive Spectral Projection for Linear System

This section focuses on how to reformulate the stochastic system via an ISP approach. The stage of constructing a deterministic system from a stochastic system via the ISP method to efficiently propagate uncertainties can be explained as follows. Given a stochastic linear system is as follows:

$$\dot{\boldsymbol{x}}(t,\xi) = \boldsymbol{A}_c(\xi)\boldsymbol{x}(t,\xi) + \boldsymbol{B}_c(\xi)\boldsymbol{u}(t) \tag{3}$$

where the state and input variables are expressed by $\boldsymbol{x} \in \mathbb{R}^{n_x}$ and $\boldsymbol{u} \in \mathbb{R}^{n_u}$ respectively, $\boldsymbol{A}_c(\xi)$ and $\boldsymbol{B}_c(\xi)$ represent the state and input matrices depending on the random variables $\xi \in \mathbb{R}$. Since the system (3) has probability uncertainty for its parameters, the state variable trajectory becomes stochastic. Meanwhile, the random variable does not affect the input variable, so it is deterministic. Furthermore, reducing the stochastic linear system to the deterministic linear system with PCEs refers to [10], [62].

Define state variables $\boldsymbol{x}(t,\xi)$, $\boldsymbol{A}_c(\xi)$ and $\boldsymbol{B}_c(\xi)$ into $x_i(t,\xi)$, $A_{c_{ij}}(\xi)$, and $B_{c_{ij}}(\xi)$ as a linear combination of the basis function $\phi_m(\xi)$, then we obtain

$$x_i(t,\xi) = \sum_{m=0}^{l_\xi} \bar{x}_{i,m}(t)\phi_m(\xi) = \bar{\boldsymbol{x}}_i(t)^T \bar{\boldsymbol{\phi}}(\xi) \tag{4}$$

$$A_{c_{ij}}(t,\xi) = \sum_{m=0}^{l_\xi} \bar{a}_{ij,m}(t)\phi_m(\xi) = \bar{\boldsymbol{a}}_{ij}{}^T \bar{\boldsymbol{\phi}}(\xi) \tag{5}$$

$$B_{c_{ij}}(t,\xi) = \sum_{m=0}^{l_\xi} \bar{b}_{ij,m}(t)\phi_m(\xi) = \bar{\boldsymbol{b}}_{ij}{}^T \bar{\boldsymbol{\phi}}(\xi) \tag{6}$$

where $\bar{\boldsymbol{x}}_i(t)$, $\bar{\boldsymbol{a}}_{ij}$, $\bar{\boldsymbol{b}}_{ij}$ and $\bar{\boldsymbol{\phi}}(\xi) \in \mathbb{R}^{p+1}$ are defined as

$$\bar{\boldsymbol{x}}_i(t) = \left[\bar{x}_{i,0}(t), \bar{x}_{i,1}(t), \cdots, \bar{x}_{i,l_\xi}(t)\right]^T,$$
$$\bar{\boldsymbol{a}}_{ij} = \left[\bar{a}_{ij,0}, \bar{a}_{ij,1}, \cdots, \bar{a}_{ij,l_\xi}\right]^T,$$
$$\bar{\boldsymbol{b}}_{ij} = \left[\bar{b}_{ij,0}, \bar{b}_{ij,1}, \cdots, \bar{b}_{ij,l_\xi}\right]^T,$$
$$\bar{\boldsymbol{\phi}}(\xi) = \left[\phi_0(\xi), \phi_1(\xi), \cdots, \phi_{l_\xi}(\xi)\right]^T$$

The coefficient $\bar{a}_{ij,m}$ and $\bar{b}_{ij,m}$ are obtained by Galerkin projection onto $\phi_m(\xi)$, $m = 0,1,\cdots,p$ given by Eqs. (7) and (8) as follows:

$$\bar{a}_{ij,m} = \frac{\langle A_{c_{ij}}(\xi),\ \phi_m(\xi)\rangle}{\langle \phi_m^2(\xi)\rangle} \tag{7}$$

$$\bar{b}_{ij,m} = \frac{\langle B_{c_{ij}}(\xi),\ \phi_m(\xi)\rangle}{\langle \phi_m^2(\xi)\rangle} \tag{8}$$

Substitute Eqs. (4), (5) and (6) into Eq. (3), so we obtain

$$\begin{aligned}\sum_{k=0}^{p} \dot{\bar{x}}_{i,k}(t)\phi_k(\xi) = &\sum_{j=1}^{n_x}\sum_{k=0}^{p}\sum_{l=0}^{p} \bar{a}_{ij,k}\,\bar{x}_{j,l}(t)\phi_k(\xi)\phi_l(\xi) \\ &+ \sum_{j=1}^{n_u}\sum_{k=0}^{p} \bar{b}_{ij,k}\,\phi_k(\xi)u_j(t).\end{aligned} \tag{9}$$

Thus, by projecting (9) onto orthogonal basis function, i.e. ϕ_m for $m = 0,\cdots,p$, and dropping the germ ξ, then Eq. (9) can be simplified to

$$\begin{aligned}\sum_{m=0}^{p} \dot{\bar{x}}_{i,m}(t)\langle\phi_m^2\rangle = &\sum_{j=1}^{n_x}\sum_{k=0}^{p}\sum_{l=0}^{p} \bar{a}_{ij,k}\,\bar{x}_{j,l}(t)\langle\phi_k\phi_l\phi_m\rangle \\ &+ \sum_{j=1}^{n_u} \bar{b}_{ij,m}\,u_j(t)\langle\phi_m^2\rangle.\end{aligned} \tag{10}$$

Then divided by $\langle\phi_m^2\rangle$, Eq. (10) becomes:

$$\begin{aligned}\dot{\bar{x}}_{i,m}(t) = &\sum_{j=1}^{n_x}\sum_{k=0}^{p}\sum_{l=0}^{p} \bar{a}_{ij,k}\,\bar{x}_{j,l}(t)C_{klm} \\ &+ \sum_{j=1}^{n_u} \bar{b}_{ij,m}\,u_j(t)\end{aligned} \tag{11}$$

where $C_{klm} = \frac{\langle\phi_k\phi_l\phi_m\rangle}{\langle\phi_m^2\rangle}$. From Eq. (11), the obtained deterministic differential equation is as follows:

$$\dot{\boldsymbol{X}}(t) = \boldsymbol{\mathcal{A}}\boldsymbol{X}(t) + \boldsymbol{\mathcal{B}}\boldsymbol{u}(t) \tag{12}$$

where $\boldsymbol{X} \in \mathbb{R}^{n_x(p+1)}$, $\boldsymbol{u} \in \mathbb{R}^{n_u}$, $\boldsymbol{\mathcal{A}} \in \mathbb{R}^{n_x(p+1)\times n_x(p+1)}$, $\boldsymbol{\mathcal{B}} \in \mathbb{R}^{n_x(p+1)\times n_u}$, and $\boldsymbol{X} = \left[\bar{\boldsymbol{x}}_1{}^T\ \bar{\boldsymbol{x}}_2{}^T\ \cdots\ \bar{\boldsymbol{x}}_{n_x}{}^T\right]^T$. Define a matrix $\boldsymbol{T}_m$ as

$$\boldsymbol{T_m} = \begin{bmatrix} C_{00m} & C_{01m} & \cdots & C_{0pm} \\ C_{10m} & C_{11m} & \cdots & C_{1pm} \\ \vdots & \vdots & \ddots & \vdots \\ C_{p0m} & C_{p1m} & \cdots & C_{ppm} \end{bmatrix}$$

The new state and input matrices, i.e., $\boldsymbol{\mathcal{A}}$ and $\boldsymbol{\mathcal{B}}$, can be defined as follows:

$$\boldsymbol{\mathcal{A}} = \left[\boldsymbol{\mathcal{A}}_{ij}\right] \text{ where } \boldsymbol{\mathcal{A}}_{ij} = \textstyle\sum_{m=0}^{p} \bar{a}_{ij,m}\boldsymbol{T}_m, i,j = 1,\ldots,n_x$$

$$\boldsymbol{\mathcal{B}} = \left[\boldsymbol{\mathcal{B}}_{ij}\right] \text{ where } \boldsymbol{\mathcal{B}} = \bar{b}_{ij}, i = 1,\ldots,n_x, j = 1,\ldots,n_u$$

The conversion of a stochastic linear system with $\boldsymbol{x} \in \mathbb{R}^{n_x}$, $\boldsymbol{u} \in \mathbb{R}^{n_u}$ using PCEs by order p, produces deterministic linear system where the states have a dimension of $n_x(p+1)$

unknown PCE coefficients for the states $\{\bar{x}_{i,m}(t)\}_{j=1,\cdots,n_x}^{m=0,\cdots,p}$. Then, Eq. (12) will be used to design the SMPC method.

III. PCE-BASED MODEL PREDICTIVE CONTROL

The polynomial chaos expansion-based MPC (PCE-MPC) is designed to realize a robust control system dealing with parameter uncertainties. The PCE approach is used to approximate the stochastic parameters in relation to a random variable with a known probability density function (pdf). The parameters approximated by PCE in a dynamical system are assumed to be time-invariant. The controller design used in this study is based on the open loop control system without chance constraints. The SMPC optimization problem, while considering the uncertain parameter in a dynamical system, can be written as follows.

Problem 1. (Stochastic MPC)

$$\min_{\boldsymbol{u}} \mathbb{E}\left[\sum_{i=1}^{N_h}(\|\boldsymbol{x}_{n+i}(\xi)\|_{\boldsymbol{Q}_x}^2 + \|\boldsymbol{u}_{n+i-1}\|_{\boldsymbol{R}_u}^2)\right] \tag{13}$$

subject to

$$\boldsymbol{x}_{n+i+1}(\xi) = \boldsymbol{A}_d(\xi)\boldsymbol{x}_{n+i}(\xi) + \boldsymbol{B}_d(\xi)\boldsymbol{u}_{n+i}, i \in [0, N_h - 1]$$
$$\boldsymbol{x}_n(\xi) = \boldsymbol{x}_0$$
$$\boldsymbol{u}_{n+i} \in \mathbb{U}, i \in [0, N_h - 1]$$

where $n = \frac{t}{T_s} \in \mathbb{N}$ is the time index, and T_s is the proper sampling time to convert a continuous-time system to a discrete-time system, $\boldsymbol{x}_n(\xi) \in \mathbb{R}^{n_x}$ and $\boldsymbol{u}_n \in \mathbb{R}^{n_u}$ denote the state and input variables in discrete-time of a linear system at time-n, respectively, $\xi \in \mathbb{R}$ represents a time-invariant parameter, $\boldsymbol{A}_d(\xi) \in \mathbb{R}^{n_x} \times \mathbb{R}^{n_x}$ and $\boldsymbol{B}_d(\xi) \in \mathbb{R}^{n_x} \times \mathbb{R}^{n_u}$ are the matrices of state and input in discrete-time, respectively, $\boldsymbol{Q}_x$ and $\boldsymbol{R}_u$ denote the positive definite matrices as the weighting factors of states and inputs, N_h is the prediction horizon, $\mathbb{U} \in \mathbb{R}^{n_u}$ declares the convex compact set of input constraints, and

$$\|\boldsymbol{x}_{n+i}(\xi)\|_{\boldsymbol{Q}_x}^2 = \boldsymbol{x}_{n+i}^T(\xi)\boldsymbol{Q}_x\boldsymbol{x}_{n+i}(\xi)$$
$$\|\boldsymbol{u}_{n+i-1}\|_{\boldsymbol{R}_u}^2 = \boldsymbol{u}_{n+i-1}^T\boldsymbol{R}_u\boldsymbol{u}_{n+i-1}$$

The optimization problem in Eq. (13) is stochastic, so it is more convenient if changed to a deterministic optimization problem using the PCEs approach. By using PCEs, for $x \in \mathbb{R}$, the quantity $\mathbb{E}[x^2]$ is approximated by

$$\begin{aligned}\mathbb{E}[x^2] &\approx \mathbb{E}\left[\sum_{i=0}^{p}\bar{x}_i\phi_i\sum_{j=0}^{p}\bar{x}_j\phi_j\right] \\ &= \mathbb{E}\left[\sum_{i=0}^{p}\sum_{j=0}^{p}\bar{x}_i\,\bar{x}_j\phi_i\,\phi_j\right]\end{aligned} \tag{14}$$

Since $\bar{x}_i$ and $\bar{x}_j$ are deterministic, Eq. (14) can be rewritten as

$$\mathbb{E}[x^2] \approx \sum_{i=0}^{p}\sum_{j=0}^{p}\bar{x}_i\,\bar{x}_j\mathbb{E}[\phi_i\phi_j] \tag{15}$$

$$\begin{aligned}&= \sum_{i=0}^{p}\sum_{j=0}^{p}\bar{x}_i\,\bar{x}_j\int_{\mathcal{D}_\xi}\phi_i\phi_j f_\xi\,d\xi \\ &= \bar{\boldsymbol{x}}^T\boldsymbol{V}\,\bar{\boldsymbol{x}}^T\end{aligned}$$

where $\mathcal{D}_\xi$ is the domain of ξ, $\bar{x}_i$ is the coefficient of polynomial ϕ_i, $f_\xi \equiv f(\xi)$ is the pdf of ξ, $\boldsymbol{V} \in \mathbb{R}^{(p+1)\times(p+1)} = v_{ij}$ is a diagonal matrix with $v_{ij} = \int_{\mathcal{D}_\xi}\phi_i\phi_j f_\xi\,d\xi = \mathbb{E}[\phi_i^2]\delta_{ij}$, i.e., $\delta_{ij} = 1$ if $i = j$ and $\delta_{ij} = 0$, if $i \neq j$, and $\bar{\boldsymbol{x}} = \left[\bar{x}_0, \bar{x}_1, \cdots, \bar{x}_p\right]^T$. Furthermore, by referring to Eq. (15), for $\boldsymbol{x} \in \mathbb{R}^{n_x}$, the quantity $\mathbb{E}[\boldsymbol{x}^T\boldsymbol{x}]$ is approximated by

$$\mathbb{E}[\boldsymbol{x}^T\boldsymbol{x}] \approx \boldsymbol{X}^T(\boldsymbol{I}_{n_x} \otimes \boldsymbol{V})\boldsymbol{X} \tag{16}$$

where the identity matrix is denoted by $\boldsymbol{I}_{n_x} \in \mathbb{R}^{n_x \times n_x}$, the Kronecker product is denoted by $\otimes$, and $\boldsymbol{X}$ is given in Eq. (12). The objective function in Eq. (13) can be derived as follows:

$$\begin{aligned}&\min_{\boldsymbol{u}} \mathbb{E}\left[\sum_{i=1}^{N_h}\left(\|\boldsymbol{x}_{n+i}(\xi)\|_{\boldsymbol{Q}_x}^2 + \|\boldsymbol{u}_{n+i-1}\|_{\boldsymbol{R}_u}^2\right)\right] \\ &= \sum_{i=1}^{N_h}\left(\mathbb{E}\left[\|\boldsymbol{x}_{n+i}(\xi)\|_{\boldsymbol{Q}_x}^2\right] + \mathbb{E}\left[\|\boldsymbol{u}_{n+i-1}\|_{\boldsymbol{R}_u}^2\right]\right)\end{aligned} \tag{17}$$

By assuming that the control inputs do not depend on the random variables and referring to Eq. (16), the objective function in Eq. (17) is rewritten in terms of PCEs as

$$\begin{aligned}&\min_{\boldsymbol{u}} \sum_{i=1}^{N_h}\left(\mathbb{E}\left[\|\boldsymbol{x}_{n+i}(\xi)\|_{\boldsymbol{Q}_x}^2\right] + \mathbb{E}\left[\|\boldsymbol{u}_{n+i-1}\|_{\boldsymbol{R}_u}^2\right]\right) \\ &\approx \min_{\boldsymbol{u}} \sum_{i=1}^{N_h}\left(\|\boldsymbol{X}_{n+i}(\xi)\|_{\boldsymbol{Q}_{\bar{x}}}^2 + \|\boldsymbol{u}_{n+i-1}\|_{\boldsymbol{R}_u}^2\right)\end{aligned} \tag{18}$$

where $\boldsymbol{Q}_{\bar{x}} = \boldsymbol{Q}_x \otimes \boldsymbol{V}$. The final reformulation of Problem 1 using PCEs can be stated below.

Problem 2. (PCE-MPC Optimization)

$$\min_{\boldsymbol{u}} \sum_{i=1}^{N_h}\left(\|\boldsymbol{X}_{n+i}(\xi)\|_{\boldsymbol{Q}_{\bar{x}}}^2 + \|\boldsymbol{u}_{n+i-1}\|_{\boldsymbol{R}_u}^2\right) \tag{19}$$

subject to

$$\boldsymbol{X}_{n+i+1} = \boldsymbol{\mathcal{A}}_d\boldsymbol{X}_{n+i} + \boldsymbol{\mathcal{B}}_d\boldsymbol{u}_{n+i}, i \in [0, N_h - 1]$$
$$\boldsymbol{X}_n = \boldsymbol{X}_0$$
$$\boldsymbol{u}_{n+i} \in \mathbb{U}, i \in [0, N_h - 1]$$

where $\boldsymbol{\mathcal{A}}_d$ dan $\boldsymbol{\mathcal{B}}_d$ are matrix forms of the discrete-time system after discretizing system (12).

Problem 2 is deterministic MPC optimization, which can be solved using the quadratic programming (QP) formula [63], [64]. By defining new variables, i.e.,

$$\bar{\boldsymbol{X}} = [\boldsymbol{X}^T \quad \boldsymbol{X}^T \quad \cdots \quad \boldsymbol{X}^T]^T \in \mathbb{R}^{n_x(p+1)N_h \times 1},$$
$$\bar{\boldsymbol{u}} = [\boldsymbol{u}^T \quad \boldsymbol{u}^T \quad \cdots \quad \boldsymbol{u}^T]^T \in \mathbb{R}^{n_u N_h \times 1},$$

the QP formulation of Problem 2 is given by Problem 3.

Problem 3. (QP of PCE-MPC Optimization)

$$\min_{\bar{\boldsymbol{u}}} \frac{1}{2}\bar{\boldsymbol{u}}^T \boldsymbol{H}\bar{\boldsymbol{u}} + \bar{\boldsymbol{u}}^T \boldsymbol{g} \tag{20}$$

subject to

$$\boldsymbol{l}_b \le \bar{\boldsymbol{u}} \le \boldsymbol{u}_b$$

where $\boldsymbol{g} = 2\boldsymbol{\beta}^T \bar{\boldsymbol{Q}}_{\bar{x}} \boldsymbol{F}\boldsymbol{X}_n \in \mathbb{R}^{n_u N_h \times 1}$

$\boldsymbol{H} = 2(\boldsymbol{\beta}^T \bar{\boldsymbol{Q}}_{\bar{x}} \boldsymbol{\beta} + \bar{\boldsymbol{R}}_u) \in \mathbb{R}^{n_u N_h \times n_u N_h}$

$\bar{\boldsymbol{Q}}_{\bar{x}} = \mathrm{diag}(\boldsymbol{Q}_{\bar{x}}, \dots, \boldsymbol{Q}_{\bar{x}}) \in \mathbb{R}^{n_x(p+1)N_h \times n_x(p+1)N_h}$

$\bar{\boldsymbol{R}}_u = \mathrm{diag}(\boldsymbol{R}_u, \dots, \boldsymbol{R}_u) \in \mathbb{R}^{n_u N_h \times n_u N_h}$

$$\boldsymbol{\beta} = \begin{bmatrix} \boldsymbol{\mathcal{B}}_d & \boldsymbol{0} & \boldsymbol{0} & \cdots & \boldsymbol{0} \\ \boldsymbol{\mathcal{A}}_d\boldsymbol{\mathcal{B}}_d & \boldsymbol{\mathcal{B}}_d & \boldsymbol{0} & \cdots & \boldsymbol{0} \\ \boldsymbol{\mathcal{A}}_d^2\boldsymbol{\mathcal{B}}_d & \boldsymbol{\mathcal{A}}_d\boldsymbol{\mathcal{B}}_d & \boldsymbol{\mathcal{B}}_d & \cdots & \boldsymbol{0} \\ \vdots & \vdots & \vdots & \ddots & \vdots \\ \boldsymbol{\mathcal{A}}_d^{N_h-1}\boldsymbol{\mathcal{B}}_d & \boldsymbol{\mathcal{A}}_d^{N_h-2}\boldsymbol{\mathcal{B}}_d & \boldsymbol{\mathcal{A}}_d^{N_h-3}\boldsymbol{\mathcal{B}}_d & \cdots & \boldsymbol{\mathcal{B}}_d \end{bmatrix}$$

$$\boldsymbol{F} = \begin{bmatrix} \boldsymbol{\mathcal{A}}_d \\ \boldsymbol{\mathcal{A}}_d^2 \\ \boldsymbol{\mathcal{A}}_d^3 \\ \vdots \\ \boldsymbol{\mathcal{A}}_d^{N_h} \end{bmatrix}, \boldsymbol{l}_b = \begin{bmatrix} \boldsymbol{u}^{min} \\ \boldsymbol{u}^{min} \\ \boldsymbol{u}^{min} \\ \vdots \\ \boldsymbol{u}^{min} \end{bmatrix}, \boldsymbol{u}_b = \begin{bmatrix} \boldsymbol{u}^{max} \\ \boldsymbol{u}^{max} \\ \boldsymbol{u}^{max} \\ \vdots \\ \boldsymbol{u}^{max} \end{bmatrix}$$

with $\boldsymbol{\beta} \in \mathbb{R}^{n_x(p+1)N_h \times n_u N_h}$, $\boldsymbol{F} \in \mathbb{R}^{n_x(p+1)N_h \times n_x(p+1)}$, $\boldsymbol{l}_b \in \mathbb{R}^{n_u N_h \times n_u N_h}$, and $\boldsymbol{u}_b \in \mathbb{R}^{n_u N_h \times n_u N_h}$. In the next section, the mathematical model of the F-16 aircraft is described to examine the proposed controller method in the presence of parametric uncertainty. To implement the PCE-MPC for the discrete-time system of (3), the algorithm is summarized as follows.

PCE-MPC algorithm

INPUT	prediction horizon N_h, weighting matrices $\boldsymbol{Q}_x$ and $\boldsymbol{R}_u$, sampling time T_s, simulation time t_f, the number of random samplings N, initial states $\boldsymbol{x}_0^s = \boldsymbol{x}_0$, $s = 1, \cdots, N$
OUTPUT	states $\boldsymbol{x}^s$ at time $n, \forall s = 1, \cdots, N$
Step 1	for $s = 1{:}\,N$
Step 2	set $n = 0$
Step 3	while $n < T = \frac{t_f}{T_s}$ do *Step 4-6*
Step 4	$\min_{\bar{\boldsymbol{u}}} \frac{1}{2}\bar{\boldsymbol{u}}^T \boldsymbol{H}\bar{\boldsymbol{u}} + \bar{\boldsymbol{u}}^T \boldsymbol{g}$ s.t. $\boldsymbol{l}_b \le \bar{\boldsymbol{u}} \le \boldsymbol{u}_b$; obtain $\bar{\boldsymbol{u}} = \{\boldsymbol{u}_{0\|n}, \cdots, \boldsymbol{u}_{N_h\|n}\}$
Step 5	$\boldsymbol{x}_{n+1}^s = \boldsymbol{A}_d(\xi^s)\boldsymbol{x}_n^s + \boldsymbol{B}_d(\xi^s)\boldsymbol{u}_{0\|n}$
Step 6	set $n = n + 1$
Step 7	OUTPUT $\{\boldsymbol{x}_n^1, \cdots, \boldsymbol{x}_n^N\}, n \in [0, T]$; STOP.

IV. NUMERICAL CASE STUDY AND DISCUSSION

The numerical example used in this simulation is the F-16 aircraft. The below equation gives the short-period mode of an F-16.

$$\dot{\boldsymbol{x}}(t,\xi) = \boldsymbol{A}_c(\xi)\boldsymbol{x}(t,\xi) + \boldsymbol{B}_c\boldsymbol{u}(t) \tag{21}$$

where the state vector is represented by $\boldsymbol{x} = [\alpha, q, x_E]^T \in \mathbb{R}^{n_x}$, the angle of attack is expressed by α, the pitch rate is symbolized by q, and the elevator state capturing actuator dynamics is denoted by x_E. The system input, $\boldsymbol{u} \in \mathbb{R}^{n_u}$, describes the elevator deflection in degrees.

The state and input matrices, $\boldsymbol{A}_c(\xi)$ and $\boldsymbol{B}_c$ in the presence of time-invariant parameter uncertainties are given by [10].

$$\boldsymbol{A}_c(\xi) = \begin{bmatrix} -0.6398 & 0.9378 & -0.0014 \\ a_{21}(\xi) & a_{22}(\xi) & a_{23}(\xi) \\ 0 & 0 & -20.2 \end{bmatrix}; \boldsymbol{B}_c = \begin{bmatrix} 0 \\ 0 \\ 20.2 \end{bmatrix}$$

where $a_{21}(\xi) = -1.5679(1 + 0.2\xi)$, $a_{22}(\xi) = -0.8791(1 + 0.2\xi)$, and $a_{23}(\xi) = -0.1137(1 + 0.2\xi)$. The values of $a_{21}(\xi)$, $a_{22}(\xi)$, and $a_{23}(\xi)$ are assumed to have a uniform distribution with 20% deviation about their nominal values. The randomness of those three parameters is governed by a single random variable, i.e., $\xi \in [-1,1]$. These uncertainties are caused by a high angle of attack that results in inaccurate aerodynamic coefficient modelling. The parameters of MPC simulation under probabilistic parameter uncertainties are summarized in Table II.

TABLE II. PARAMETERS OF MPC SIMULATION

Parameter	Value	Unit
$\boldsymbol{T_s}$	0.01	s
$\boldsymbol{N_h}$	20 (equivalent to 0.2 s)	N/A
$\boldsymbol{u_{min}}$	-25	deg
$\boldsymbol{u_{max}}$	25	deg
$\boldsymbol{R_u}$	1	N/A
$\boldsymbol{Q_x}$	diag(10,1000,1)	N/A
$\boldsymbol{x_0}$	$(35, 0, 0)^T$	N/A

PCE-MPC aims to stabilize the pitch rate and angle of attack variables while satisfying the elevator constraint due to uncertain parameters in the system model. The observed state variables in this study are the angle of attack and pitch rate variables. By referring to Table I, the Legendre polynomials are employed to formulate the PCEs. The order of PCEs is set to $p = 1, 2, 3,$ and 4, resulting in $p + 1$ terms in the expansion. The Galerkin projection method is used to compute polynomial coefficients. The inner product is approximated using numerical integration, namely Gauss-Legendre quadrature [65] with $2p^3 - 1$ quadrature points since there is inner product calculation, $\langle \phi_k \phi_l \phi_m \rangle$ resulting p^3 order, should be evaluated. The simulation is performed using MATLAB R2021a on a computer with 8GB RAM and a core i5 processor. The errors of mean and variance values for each state variable at time t can be computed by

$$\boldsymbol{\varepsilon}_\mu(t) = \left|\frac{\boldsymbol{\mu}(t) - \boldsymbol{\mu}_{exact}(t)}{\boldsymbol{\mu}_{exact}(t)}\right|, \text{ and } \boldsymbol{\varepsilon}_\sigma(t) = \left|\frac{\boldsymbol{\sigma}(t) - \boldsymbol{\sigma}_{exact}(t)}{\boldsymbol{\sigma}_{exact}(t)}\right|$$

where $\boldsymbol{\mu}_{exact}(t)$ and $\boldsymbol{\sigma}_{exact}(t)$ denote the exact values of mean and variance at time t. The exact values of mean and variance are calculated as follows.

$$\boldsymbol{\mu}_{exact} = \mathbb{E}[\boldsymbol{x}]$$

$$\boldsymbol{\sigma}_{exact} = \mathrm{diag}(\mathbb{E}[(\boldsymbol{x} - \boldsymbol{\mu}_{exact})(\boldsymbol{x} - \boldsymbol{\mu}_{exact})^T])$$

where $\mathbb{E}[\boldsymbol{x}] = \int_{\mathcal{D}_\xi} \boldsymbol{x} f_\xi \, d\xi$ and the exact solution of system (21) is given by

$$\boldsymbol{x}(t) = e^{\boldsymbol{A}_c(\xi)t}\boldsymbol{x}_0 + \int_0^t e^{\boldsymbol{A}_c(\xi)(t-\tau)}\boldsymbol{B}_c\boldsymbol{u}(\tau)d\tau$$

The errors of mean and variance for the angle of attack and pitch rate due to propagating the uncertainty are shown in Fig. 1.

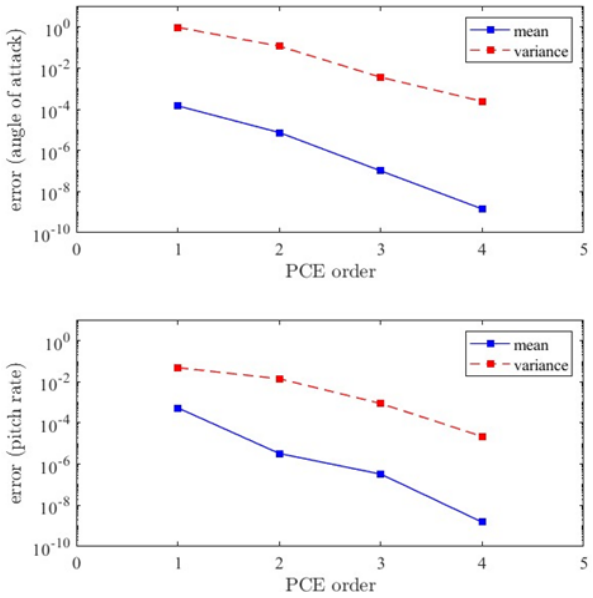

Fig. 1. Error convergence of angle of attack (top) and pitch rate (bottom) in stochastic system (21) over simulation time of 10 s. The displayed results are at time 10 s computed using $\boldsymbol{u} = 25°$

Fig. 1 illustrates the errors in mean and variance for the angle of attack and pitch rate variables concerning the PCE order. It is evident that as the polynomial degree increases, the error values for both the mean and variance of the angle of attack and pitch rate decrease. The system described by Eq. (21) is solved using a 4th-order Runge-Kutta method over a simulation time of 10 seconds for a specific input. However, due to the escalating dimensionality associated with higher-degree polynomials and the marginal reduction in mean and variance errors, the PCE is truncated at the fourth order.

To assess the effectiveness of PCE in predicting the mean and variance of state variables, a comparison is made with the Monte Carlo method. The errors in predicting the mean and variance for the angle of attack and pitch rate are presented in Fig. 2.

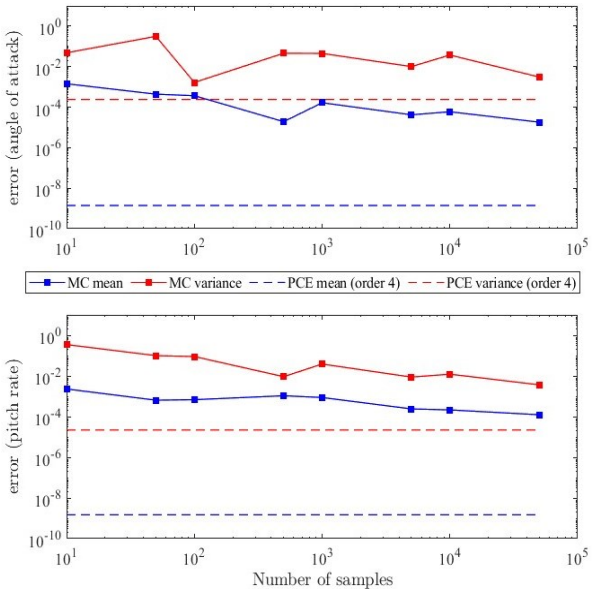

Fig. 2. The error comparisons in predicting the mean and variance of angle of attack (top) and pitch rate (bottom) with respect to Monte Carlo samples over simulation time of 10 s. The displayed results are at time 10 s using the same input

Fig. 2 shows the mean and variance produced by the PCE. The errors of 4th-order PCE are smaller than Monte Carlo method both angle of attack and pitch rate. For the information, the PCE only needs 5 samples to obtain better accuracy in predicting the mean and variance. Even though the Monte Carlo method uses 50.000 samples it cannot yield the same accuracy as PCE on a 4th-order basis. On the other hand, increasing the number of samples in Monte Carlo can influence a computational burden. In contrast to the 4th-order PCE, it only needs 3.02 s for solving the system (12) using the Runge-Kutta method. The computational time with the different number of samples is shown in Table III.

TABLE III. COMPUTATIONAL TIME OF MONTE CARLO WITH THE DIFFERENT NUMBER OF SAMPLES

Number of samples	Computational time (s)
10	0.09
50	0.33
100	0.55
500	2.73
1000	4.61
5000	21.70
10000	43.33
50000	223.35

A. PCE-MPC Simulations

To tackle the sensitivity of PCE-MPC under varying initial conditions, we establish two simulation variations as follows.

- Scenario 1: $\boldsymbol{x_0} = (35,0,0)^T$
- Scenario 2: $\boldsymbol{x_0} = (-10,-10,0)^T$

Based on the obtained results previously, the PCE-MPC is designed using a fourth-order basis. The optimal inputs by solving the QP optimization (20) of the PCE-MPC problem (19) under various initial conditions are shown in Fig. 3.

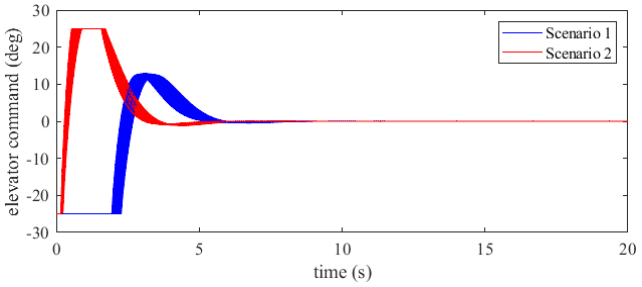

Fig. 3. Optimal inputs by solving the PCE-MPC optimization in (19) using quadratic programming under 1000 Monte Carlo simulation runs

Fig. 3 shows the proposed method can satisfy the given input constraints, $|\boldsymbol{u}(t)| \leq 25°$. The elevator adjustment in the beginning time can be caused by the controller's way of returning the angle of attack from the initial values to the original points. Using the control input depicted in Fig. 3, the angle of attack and pitch rate trajectories under 1000 Monte Carlo simulation runs with different initial conditions are shown in Fig. 4.

Fig. 4 displays the pitch rate and angle of attack responses with different initial conditions calculated among 1000 samples of $a_{21}(\xi)$, $a_{22}(\xi)$, and $a_{23}(\xi)$ as a function of ξ. Based on Fig. 4, it's evident that PCE-MPC demonstrates

robust performance as both the angle of attack and pitch rate responses converge to their original values in both scenario 1 and scenario 2.

Fig. 5 illustrates histograms of the angle of attack and pitch rate at 5 s, 10 s, 15 s, and 20 s under different initial conditions. From Fig. 5, it is apparent that both the angle of attack and pitch rate exhibit minimal variance initially, which diminishes over time, approaching zero. This indicates that PCE-MPC effectively mitigates the impact of parameter uncertainties in the dynamical system, ensuring convergence to the original points across all uncertainty realizations, as depicted in Fig. 5.

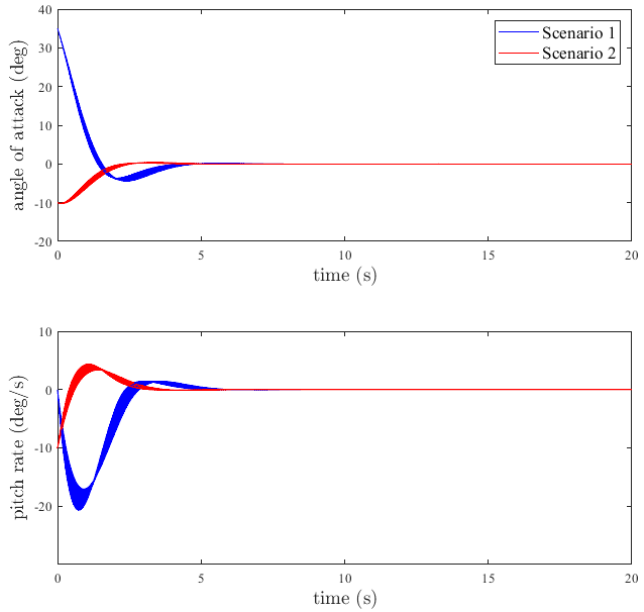

Fig. 4. The angle of attack and pitch rate response with parameter realizations calculated under 1000 Monte Carlo simulation runs and various initial conditions

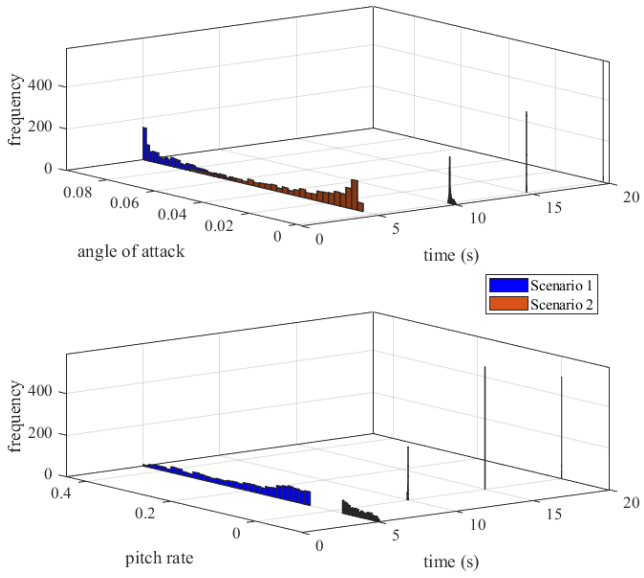

Fig. 5. Histograms of the angle of attack (top) and pitch rate (bottom) under 1000 Monte Carlo simulation runs and various initial conditions at different time

Fig. 4 displays the pitch rate and angle of attack responses with different initial conditions calculated among 1000 samples of $a_{21}(\xi)$, $a_{22}(\xi)$, and $a_{23}(\xi)$ as a function of ξ. Based on Fig. 4, it's evident that PCE-MPC demonstrates robust performance as both the angle of attack and pitch rate responses converge to their original values in both scenario 1 and scenario 2.

Fig. 5 illustrates histograms of the angle of attack and pitch rate at 5 s, 10 s, 15 s, and 20 s under different initial conditions. From Fig. 5, it is apparent that both the angle of attack and pitch rate exhibit minimal variance initially, which diminishes over time, approaching zero. This indicates that PCE-MPC effectively mitigates the impact of parameter uncertainties in the dynamical system, ensuring convergence to the original points across all uncertainty realizations, as depicted in Fig. 5.

B. Comparison Between MPC and PCE-MPC

To assess the performance of PCE-MPC, it is crucial to compare it with standard MPC. We ensure a fair comparison by setting identical initial conditions and controller parameters between PCE-MPC and standard MPC. The results of this comparison are presented in Fig. 6 and Fig. 7, illustrating state responses and histograms, respectively.

Fig. 6 and Fig. 7 depict that both MPC and PCE-MPC exhibit negligible differences, showcasing nearly identical performance. Overall, the effectiveness of these control methods hinges on system conditions and uncertainties. In this scenario, the comparable performance between MPC and PCE-MPC may be attributed to factors like the system's uncertainties not significantly impacting the performance of SMPC, and the system itself being relatively simple without a complex uncertainty structure. The computational complexity between MPC and PCE-MPC is given in Table IV.

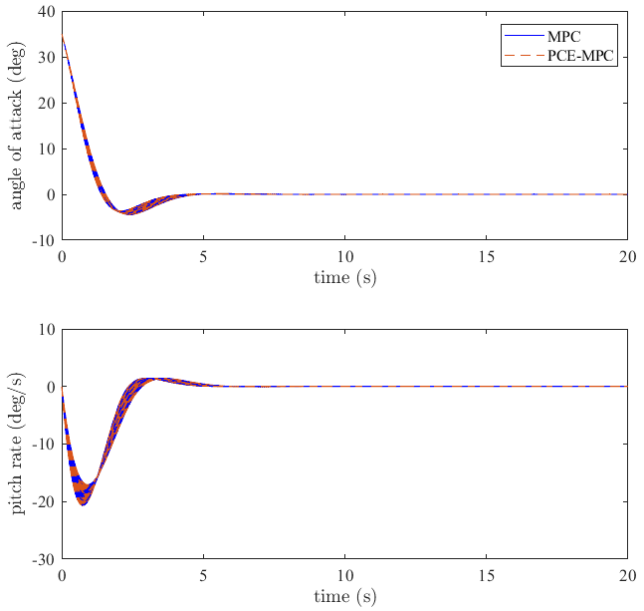

Fig. 6. The angle of attack and pitch rate responses between MPC and PCE-MPC under 1000 Monte Carlo simulation runs

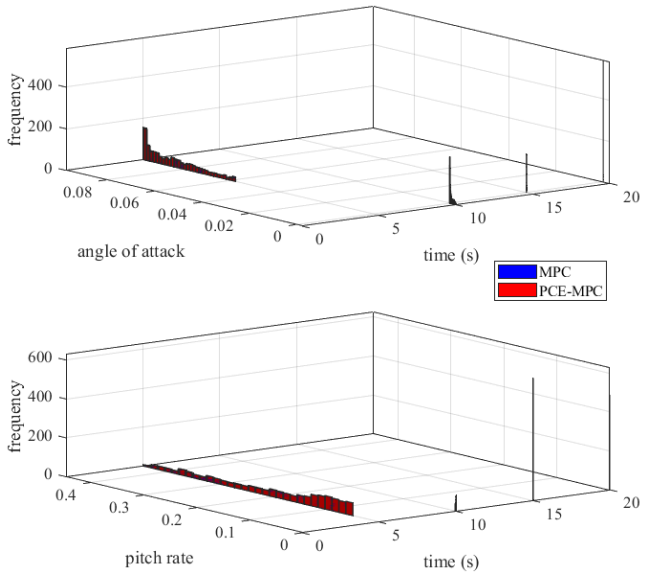

Fig. 7. The angle of attack and pitch rate histograms of MPC and PCE-MPC under 1000 Monte Carlo simulation runs at different time

TABLE IV. COMPUTATIONAL TIME BETWEEN MPC AND PCE-MPC FOR EACH RANDOM SAMPLING

Methods	Computational time (s)
MPC	8.97
PCE-MPC	9.76

Table IV examines the time taken to solve MPC and PCE-MPC optimizations using QP for each random sampling. It is evident that MPC exhibits lower computational complexity compared to PCE-MPC. This is attributed to the higher dimensionality of the system when employing the PCE method with the ISP approach to construct a deterministic system.

V. CONCLUSION

This paper effectively showcases the design and application of PCE-MPC in the presence of time-invariant probabilistic parameters. Initially, the system with probabilistic parameters undergoes conversion into a deterministic one via an ISP approach. This transformation results in a system dimension larger than the original so that it affects computational efficiency. The accuracy of PCE in predicting the mean and variance of state variables is compared to the Monte Carlo method. The controller design proposed relies on a surrogate model, established through the PCE approach under assumptions outlined in Section III. The QP framework is utilized to obtain optimal control inputs by solving the surrogate optimization problem constructed using the PCE method. The practical demonstration of the proposed controller focuses on the short-period mode of the F-16 aircraft. The simulation results indicate that PCE-MPC effectively stabilizes angle of attack and pitch rate responses under parameter uncertainty across various initial conditions. Considering the complexity concerns, it is recommended to scrutinize the computational efficiency of the proposed method using the QP framework and alternative approaches. Furthermore, revisiting the comparison between MPC and PCE-MPC, this time incorporating a more complex system like longitudinal model dynamics, is advisable. Another potential challenge lies in integrating chance constraints of the states into the PCE-MPC method, as in certain cases, considering state constraints is vital in controller design processes. By utilizing chance constraints, violations of state constraints can be mitigated. In the aerospace field, external disturbances such as turbulence should be considered in actual implementation. Additionally, the PCE-MPC method represents a significant advancement in predictive control, offering promising applications not only in aerospace but also in fields like chemical processes and finance where parameter uncertainties are prevalent.

ACKNOWLEDGMENT

This research received funding from the Ministry of Education, Culture, Research and Technology (KEMENDIKBUDRISTEK) through the Indonesian Education Scholarship (BPI) for the Doctoral Study Completion scheme in 2023. The authors are also grateful to the anonymous reviewers for their comments and suggestions, which have contributed to the improvement of this manuscript.

REFERENCES

[1] V. B. V. Nghia, T. Van Thien, N. N. Son, and M. T. Long, "Adaptive neural sliding mode control for two wheel self balancing robot," *Int. J. Dyn. Control*, vol. 10, no. 3, pp. 771–784, 2022.

[2] D. T. Tran, N. M. Hoang, N. H. Loc, Q. T. Truong, and N. T. Nha, "A Fuzzy LQR PID Control for a Two-Legged Wheel Robot with Uncertainties and Variant Height," *J. Robot. Control*, vol. 4, no. 5, pp. 612–620, 2023.

[3] Y. Wan, D. E. Shen, S. Lucia, R. Findeisen, and R. D. Braatz, "A Polynomial Chaos Approach to Robust Static Output-Feedback Control With Bounded Truncation Error," *IEEE Trans. Automat. Contr.*, vol. 68, no. 1, pp. 470–477, 2022.

[4] W. Sun, S.-F. Su, J. Xia, and Y. Wu, "Adaptive tracking control of wheeled inverted pendulums with periodic disturbances," *IEEE Trans. Cybern.*, vol. 50, no. 5, pp. 1867–1876, 2018.

[5] S. Subramanian, S. Lucia, R. Paulen, and S. Engell, "Tube-enhanced multi-stage model predictive control for flexible robust control of constrained linear systems with additive and parametric uncertainties," *Int. J. Robust Nonlinear Control*, vol. 31, no. 9, pp. 4458–4487, 2021.

[6] R. Jaiswal and O. Prakash, "Classical and Modern gain estimation approach of PID controller for the pitch control of the RCTA aircraft," *INCAS Bull.*, vol. 14, no. 1, pp. 39–56, 2022.

[7] W. Ahmed, Z. Li, H. Maqsood, and B. Anwar, "System modeling and controller design for lateral and longitudinal motion of F-16," *Autom. Control Intell. Syst.*, vol. 7, no. 1, pp. 39–45, 2019.

[8] G. P. Dos Santos, A. Kossoski, J. M. Balthazar, and A. M. Tusset, "SDRE and LQR Controls Comparison Applied in High-Performance Aircraft in a Longitudinal Flight," *Int. J. Robot. Control Syst.*, vol. 1, no. 2, pp. 131–144, 2021.

[9] S. Ijaz, C. Fuyang, M. Tariq, and H. Anwaar, "Adaptive integral-sliding-mode control strategy for maneuvering control of F16 aircraft subject to aerodynamic uncertainty," *Appl. Math. Comput.*, vol. 402, pp. 1–25, 2021, doi: 10.1016/j.amc.2021.126053.

[10] J. Fisher and R. Bhattacharya, "Linear quadratic regulation of systems with stochastic parameter uncertainties," *Automatica*, vol. 45, no. 12, pp. 2831–2841, 2009.

[11] J. Köhler, R. Soloperto, M. A. Müller, and F. Allgöwer, "A computationally efficient robust model predictive control framework for uncertain nonlinear systems," *IEEE Trans. Automat. Contr.*, vol. 66, no. 2, pp. 794–801, 2020.

[12] Y. Yang, H. Xu, and X. Yao, "Disturbance rejection event-triggered robust model predictive control for tracking of constrained uncertain robotic manipulators," *IEEE Trans. Cybern.*, 2023.

[13] O. Khan, G. Mustafa, A. Q. Khan, and M. Abid, "Robust observer-based model predictive control of non-uniformly sampled systems," *ISA Trans.*, vol. 98, pp. 37–46, 2020.

[14] A. Kapnopoulos, C. Kazakidis, and A. Alexandridis, "Quadrotor trajectory tracking based on backstepping control and radial basis function neural networks," *Results Control Optim.*, vol. 14, p. 100335, 2024.

[15] I. Lopez-Sanchez, R. Pérez-Alcocer, and J. Moreno-Valenzuela, "Trajectory tracking double two-loop adaptive neural network control for a Quadrotor," *J. Franklin Inst.*, vol. 360, no. 5, pp. 3770–3799, 2023.

[16] L. Roveda and D. Piga, "Robust state dependent Riccati equation variable impedance control for robotic force-tracking tasks," *Int. J. Intell. Robot. Appl.*, vol. 4, pp. 507–519, 2020.

[17] R. Bhattacharya, "Robust LQR design for systems with probabilistic uncertainty," *Int. J. Robust Nonlinear Control*, vol. 29, no. 10, pp. 3217–3237, 2019.

[18] M. F. von Andrian-Werburg, "Fast Stochastic Model Predictive Control Under Parametric Uncertainties," *Massachusetts Institute of Technology, Department of Chemical Engineering*, 2020.

[19] Y. Wan, D. E. Shen, S. Lucia, R. Findeisen, and R. D. Braatz, "Polynomial chaos-based H2 output-feedback control of systems with probabilistic parametric uncertainties," *Automatica*, vol. 131, p. 109743, 2021.

[20] A. Mesbah, I. V Kolmanovsky, and S. Di Cairano, "Stochastic model predictive control," *Handb. Model Predict. Control*, pp. 75–97, 2019.

[21] F. Petzke, A. Mesbah, and S. Streif, "Pocet: a polynomial chaos expansion toolbox for matlab," *IFAC-PapersOnLine*, vol. 53, no. 2, pp. 7256–7261, 2020.

[22] T. L. M. Santos, V. M. Cunha, and A. Mesbah, "Stochastic model predictive control with adaptive chance constraints based on empirical cumulative distributions," *IFAC-PapersOnLine*, vol. 53, no. 2, pp. 11257–11263, 2020.

[23] L. Xia, S. Yuan, Z. Zou, and L. Zou, "Uncertainty quantification of hydrodynamic forces on the DTC model in shallow water waves using CFD and non-intrusive polynomial chaos method," *Ocean Eng.*, vol. 198, p. 106920, 2020.

[24] S. Hijazi, G. Stabile, A. Mola, and G. Rozza, "Non-intrusive polynomial chaos method applied to full-order and reduced problems in computational fluid dynamics: A comparison and perspectives," *Quantif. Uncertain. Improv. Effic. Technol. QUIET Sel. Contrib.*, pp. 217–240, 2020.

[25] N. El Moçayd and M. Seaid, "Data-driven polynomial chaos expansions for characterization of complex fluid rheology: Case study of phosphate slurry," *Reliab. Eng. & Syst. Saf.*, vol. 216, p. 107923, 2021.

[26] M. Lacour, G. Bal, and N. Abrahamson, "Dynamic stochastic finite element method using time-dependent generalized polynomial chaos," *Int. J. Numer. Anal. Methods Geomech.*, vol. 45, no. 3, pp. 293–306, 2021.

[27] E. Voelsen, M. M. Dannert, A. A. Basmaji, F. Bensel, and U. Nackenhorst, "Sparse polynomial chaos expansion for nonlinear finite element simulations with random material properties," *PAMM*, vol. 23, no. 1, p. e202200131, 2023.

[28] L. Chen, J. Zhao, H. Li, Y. Huang, and X. Yuan, "A Polynomial Chaos Expansion Method for Mechanical Properties of Flexoelectric Materials Based on the Isogeometric Finite Element Method," *Sustainability*, vol. 15, no. 4, p. 3417, 2023.

[29] J.-J. Sinou and E. Denimal, "Reliable crack detection in a rotor system with uncertainties via advanced simulation models based on kriging and Polynomial Chaos Expansion," *Eur. J. Mech.*, vol. 92, p. 104451, 2022.

[30] A. A. Basmaji, A. Fau, J. H. Urrea-Quintero, M. M. Dannert, E. Voelsen, and U. Nackenhorst, "Anisotropic multi-element polynomial chaos expansion for high-dimensional non-linear structural problems," *Probabilistic Eng. Mech.*, vol. 70, p. 103366, 2022.

[31] P. S. Palar, L. R. Zuhal, and K. Shimoyama, "Global Sensitivity Analysis in Aerodynamic Design using Shapley Effects and Polynomial Chaos Regression," *IEEE Access*, vol. 11, pp. 114825-114839, 2023.

[32] Y. Li, H. Si, X. Wu, W. Zhao, G. Li, and J. Qiu, "Uncertainty quantification analysis with arbitrary polynomial chaos method: Application in slipstream effect of propeller aircraft," *Mod. Phys. Lett. B*, p. 2350049, 2023.

[33] Z. Wang, L. Wang, X. Wang, Q. Sun, and G. Yang, "Propagation algorithm for hybrid uncertainty parameters based on polynomial chaos expansion," *Int. J. Numer. Methods Eng.*, vol. 124, no. 19, pp. 4203–4223, 2023.

[34] X. Zhu and B. Sudret, "Stochastic polynomial chaos expansions to emulate stochastic simulators," *Int. J. Uncertain. Quantif.*, vol. 13, no. 2, 2023.

[35] M. M. Dannert, F. Bensel, A. Fau, R. M. N. Fleury, and U. Nackenhorst, "Investigations on the restrictions of stochastic collocation methods for high dimensional and nonlinear engineering applications," *Probabilistic Eng. Mech.*, vol. 69, p. 103299, 2022.

[36] A. Chordia and J. N. Tripathi, "Uncertainty quantification of rf circuits using stochastic collocation techniques," *IEEE Electromagn. Compat. Mag.*, vol. 11, no. 1, pp. 45–56, 2022.

[37] X. Sun, X. Pan, and J.-I. Choi, "Non-intrusive framework of reduced-order modeling based on proper orthogonal decomposition and polynomial chaos expansion," *J. Comput. Appl. Math.*, vol. 390, p. 113372, 2021.

[38] J. Son and Y. Du, "Comparison of intrusive and nonintrusive polynomial chaos expansion-based approaches for high dimensional parametric uncertainty quantification and propagation," *Comput. \& Chem. Eng.*, vol. 134, p. 106685, 2020.

[39] B. Debusschere. *Intrusive Polynomial Chaos Methods for Forward Uncertainty Propagation* (No. SAND2015-9250B). Sandia National Lab.(SNL-CA), 2015.

[40] D. Shen, H. Wu, B. Xia, and D. Gan, "Polynomial chaos expansion for parametric problems in engineering systems: A review," *IEEE Syst. J.*, vol. 14, no. 3, pp. 4500–4514, 2020.

[41] M. Behtash and M. J. Alexander-Ramos, "A Reliability-Based Formulation for Simulation-Based Control Co-Design Using Generalized Polynomial Chaos Expansion," *J. Mech. Des.*, vol. 144, no. 5, p. 51705, 2022.

[42] Z. Ma, H. Schlüter, F. Berkel, T. Specker, and F. Allgöwer, "Recursive Feasibility and Stability for Stochastic MPC based on Polynomial Chaos," *IFAC-PapersOnLine*, vol. 56, no. 1, pp. 204–209, 2023.

[43] R. Ou, J. Schießl, M. H. Baumann, L. Grüne, and T. Faulwasser, "A Polynomial Chaos Approach to Stochastic LQ Optimal Control: Error Bounds and Infinite-Horizon Results," *arXiv Prepr. arXiv2311.17596*, 2023.

[44] L. Nechak, H.-F. Raynaud, and C. Kulcsár, "Stochastic linear quadratic control via random parameter-dependent truncated balanced realization," *Int. J. Robust Nonlinear Control*, vol. 31, no. 4, pp. 1208–1226, 2021.

[45] Y. Chen, Y. Song, L. Shi, and J. Gao, "Stochastic model predictive control for driver assistance control of intelligent vehicles considering uncertain driving environment," *J. Vib. Control*, vol. 29, no. 3–4, pp. 758–771, 2023.

[46] S. Mosharafian and J. M. Velni, "A hybrid stochastic model predictive design approach for cooperative adaptive cruise control in connected vehicle applications," *Control Eng. Pract.*, vol. 130, p. 105383, 2023.

[47] R. D. McAllister and J. B. Rawlings, "On the inherent distributional robustness of stochastic and nominal model predictive control," *IEEE Trans. Automat. Contr.*, vol. 69, no. 2, pp. 741-754, 2023.

[48] M. H. Baumann and L. Grüne, "Does the effort of Monte Carlo pay off? A case study on stochastic MPC," *IFAC-PapersOnLine*, vol. 54, no. 6, pp. 70–75, 2021.

[49] M. E. Sezgin, S. Pouraltafi-Kheljan, M. Beyarslan, and M. Göl, "Stochastic Model Predictive Control for Microgrids Based on Monte Carlo Simulations," in *2022 57th International Universities Power Engineering Conference (UPEC)*, pp. 1–6, 2022.

[50] J. A. Paulson and A. Mesbah, "An efficient method for stochastic optimal control with joint chance constraints for nonlinear systems," *Int. J. Robust Nonlinear Control*, vol. 29, no. 15, pp. 5017–5037, 2019.

[51] J. A. Paulson, E. A. Buehler, R. D. Braatz, and A. Mesbah, "Stochastic model predictive control with joint chance constraints," *Int. J. Control*, vol. 93, no. 1, pp. 126–139, 2020.

[52] A. Pozzi and D. M. Raimondo, "Stochastic model predictive control for optimal charging of electric vehicles battery packs," *J. Energy Storage*, vol. 55, p. 105332, 2022.

[53] M. von Andrian and R. D. Braatz, "Fast stochastic model predictive control of unstable dynamical systems," *IFAC-PapersOnLine*, vol. 53, no. 2, pp. 7262–7267, 2020.

[54] T. Asfihani, S. Subchan, D. M. Rosyid, and A. Sulisetyono, "Dubins Path Tracking Controller of USV using Model Predictive Control in Sea Field," *J. Eng. Appl. Sci.*, vol. 14, no. 20, pp. 7778–7787, 2019.

[55] H. Purnawan, T. Asfihani, and S. Subchan, "Disturbance Observer Model Predictive Control with Application to UAV Pitch Angle Control," *AIP Conference Proceedings*, vol. 2641, no. 1, 2021.

[56] C. S. Agustina, T. Asfihani, R. R. Ginting, and S. Subchan, "Model predictive control in optimizing stock portfolio based on stock prediction data using Holt-Winter's exponential smoothing," in *Journal of Physics: Conference Series*, vol. 1821, no. 1, p. 12030, 2021.

[57] N. Wiener, "The homogeneous chaos," *Am. J. Math.*, vol. 60, no. 4, pp. 897–936, 1938.

[58] P. Bonnaire, P. Pettersson, and C. F. Silva, "Intrusive generalized polynomial chaos with asynchronous time integration for the solution of the unsteady Navier--Stokes equations," *Comput. & Fluids*, vol. 223, p. 104952, 2021.

[59] R. Zhang and H. Dai, "Independent component analysis-based arbitrary polynomial chaos method for stochastic analysis of structures under limited observations," *Mech. Syst. Signal Process.*, vol. 173, p. 109026, 2022.

[60] C. Eckert, M. Beer, and P. D. Spanos, "A polynomial chaos method for arbitrary random inputs using B-splines," *Probabilistic Eng. Mech.*, vol. 60, p. 103051, 2020.

[61] N. Lüthen, S. Marelli, and B. Sudret, "Sparse polynomial chaos expansions: Literature survey and benchmark," *SIAM/ASA J. Uncertain. Quantif.*, vol. 9, no. 2, pp. 593–649, 2021.

[62] J. A. Paulson, A. Mesbah, S. Streif, R. Findeisen, and R. D. Braatz, "Fast stochastic model predictive control of high-dimensional systems," in *53rd IEEE Conference on decision and Control*, pp. 2802–2809, 2014.

[63] H. Purnawan, T. Asfihani, and S. Subchan, "Disturbance observer model predictive control with application to UAV pitch angle control," in *AIP Conference Proceedings*, 2022, vol. 2641, no. 1, p. 30015.

[64] P. Otta, O. Šantin, and V. Havlena, "On the quadratic programming solution for model predictive control with move blocking," in *2021 23rd International Conference on Process Control (PC)*, pp. 49–54, 2021.

[65] L. Wang, Z. Chen, and G. Yang, "A polynomial chaos expansion approach for nonlinear dynamic systems with interval uncertainty," *Nonlinear Dyn.*, vol. 101, no. 4, pp. 2489–2508, 2020.